RSC Advances

Characteristics and kinetics of biomass tar cracking in a Micro Fluidized Bed

Journal:	*RSC Advances*
Manuscript ID	RA-ART-07-2015-013323.R1
Article Type:	Paper
Date Submitted by the Author:	11-Sep-2015
Complete List of Authors:	Mao, Yebing; Shandong University, Dong, Yuping; Shandong University, Wang, Bin; Shandong University, Chang, Jiafu; Shandong Baichuan Tongchuan Energy Co. Ltd., Yu, Jie; Shandong Baichuan Tongchuan Energy Co. Ltd., Zhang, Yi; Shandong Baichuan Tongchuan Energy Co. Ltd., Huo, Yan; Shandong Baichuan Tongchuan Energy Co. Ltd., Sun, Chuansheng; Shandong Baichuan Tongchuan Energy Co. Ltd.,

Characteristics and kinetics of biomass tar cracking in a Micro Fluidized Bed

Yebing Mao[a], Yuping Dong[a]*, Bin Wang[a], Jiafu Chang[b], Jie Yu[b], Yi Zhang[b], Yan Huo[b], Chuansheng Sun[b]

[a] Key Laboratory of High-efficiency and Clean Mechanical Manufacture of Ministry of Education, School of Mechanical Engineering, Shandong University, Jinan 250061, P. R. China

[b] Shandong Baichuan Tongchuan Energy Co. Ltd., Jinan 250101, P. R. China

Corresponding author: Tel./fax: +86 531 88392199, E-mail address: dongyp@sdu.edu.cn (Y. Dong).

Abstract: This study is devoted to investigate characteristics and kinetics of biomass tar cracking in a micro fluidized bed reactor for liquid (MFBRL). The carbon balance and conversion were measured to estimate the performance of MFBRL, and the results showed good reproducibility and reliability. H_2, CH_4 and CO comprised the vast bulk of producer gas and the total volume fraction of them increased from 69.85% to 93.62% (973-1173 K). Kinetic parameters, including reaction order, pre-exponential factor and apparent activation energy, were studied with isothermal method. The reaction orders varied greatly with temperatures, suggesting that temperature significantly affected the reaction mechanism. The pre-exponential factors for H_2, CH_4, CO and gas mixture were in the range of $2.37*10^3$-$2.87*10^5$ S^{-1}, while the apparent activation energies of them ranged from 62.96-100.2 kJ/mol. Compared to the fixed bed experiments, the derived results were obvious higher, indicating the kinetic parameters were more suitable for

describing the intrinsic reactions.

Key words: Micro Fluidized Bed Reaction; Biomass tar; Tar cracking; Kinetic parameters; Isothermal reaction.

1. Introduction:

Biomass gasification is considered as one of the most promising biomass conversion technologies. However, the formation of tar during gasification cannot be ignored[1]. Tar is viewed as one of the most undesirable byproducts of gasification because of various followed problems. Tar not only causes a waste of energy[2], but also tends to make catalyst poisoning, resulting in increasing difficulties in gas synthesizing. Furthermore, the condensation of tar endangers the gasification equipment, as well as the downstream equipments such as engines and turbines[3]. In addition, a large number of carcinogens in tar also pose a serious threat to the environment and human health. Hence, tar removal is the key issue for a successful application of biomass-derived producer gas. Compared to physical methods, cracking methods are more efficient and clearer by way of converting tar into small molecular gas [4-6], especially the catalytic cracking method which can achieve high purity at relatively low temperature.

Tar cracking contains a series of complicated physical and chemical changes. It is incapable of taking the corresponding prediction, diagnosis and treatment measures for possible problems in engineering application without a thorough understanding of reaction mechanism. Kinetics analysis, which was usually conducted in TGA (thermogravimetric analyzer) or self-made devices[7-9], can reveal the relationship

between reaction rate and its influence factor such as temperature, concentration, mass transfer, as well as the resulting variation. Accurate kinetic parameters contribute to a deeper understanding of the reaction mechanism. In recent years, TGA is widely used in the reaction characteristics and kinetics analysis due to the advantage of high sensitivity and accurate reaction condition. But owing to the limited heating rate (usually <100 K/min), the sample has to undergo a long heating process. The mass loss, which was resulted from the evaporation of the volatile components during the heating process rather than reactions, would lead to deviation between the results and the actual condition. Moreover, the reactions are vulnerable to be affected by diffusion inhibition in the TGA, consequently making the deduced kinetic parameters deviate from the intrinsic reaction. Hence, it's inappropriate to analyze tar cracking using TGA. Also some researchers designed self-made experimental devices such as fluidized bed and fixed bed. However, the reactors used are not standardized and usually large in size. Since in large reactors the reaction conditions of different zones are quite different while the influence factors of tar cracking are diverse and complex, it is difficult to reveal the differential characteristics and the intrinsic kinetics of tar cracking directly in large reactors.

The isothermal differential characteristics of micro fluidized bed reaction (MFBR) have been verified in the gas-solid reactions[10, 11]. Obviously, fluidized beds enable the considerable good mixing, heat and mass transfer, so the diffusion inhibition is minimized[12]. Besides, the online feed combined with rapid heating of MFBR may

potentially offer an approach of avoiding the mass loss caused by volatilization. Thus, the MFBR is a potential ideal equipment to analyze the reaction of liquid feedstock. However, there are no studies to demonstrate its availability for liquid feedstock. Moreover, MFBR cannot feed liquid feedstock online. To address the deficiency of MFBR in liquid phase reaction analysis, Shandong University and Shandong Baichuan Tongchuang Energy Co. Ltd developed the micro fluidized bed reactor for liquid (MFBRL). In this paper, tar cracking experiments was conducted in a MFBRL to study the characteristics and kinetics of biomass tar cracking. The authors preliminarily investigated the cracking mechanism and calculated the kinetics parameters of tar cracking reaction. Parallel tests using a fixed bed reactor were conducted to further estimate the applicability of MFBRL to liquid sample. The authors hope that the MFBRL can provide a new approach for the analysis of reaction of liquid sample. It is also expected that the present study can provide theoretical basis and parameters support for optimizing tar removal technology and reactor design.

2. Experimental

The sample used in the experiments is biomass tar, and its ultimate analysis is shown in Table 1.

Table 1 Ultimate analysis of biomass tar

Sample	Ultimate analysis (wt. %, dry basis)					
	C	H	N	S	O	total
Tar	79.48	9.19	0.78	0.24	10.31	100

The scheme diagram of the experimental system is demonstrated in Fig. 1, consisting of a quartz tube reactor, a sampling device, a detection device and certain necessary control devices. Compared to the reactor used for gas-solid reaction[13], the reactor adopted in this study has a higher main reaction zone of 80 mm in height for the sake of prolonging the residence time in the main reaction zone. Accordingly, some adjustments were made to the furnace to ensure the temperature of the main reaction zone. In order to avoid the tar feedstock adhering to the wall of the inlet, the sample was injected into the main reaction zone directly by combination device of a syringe and an injection pump, which was comprised of a stepping motor and ball screw injector.

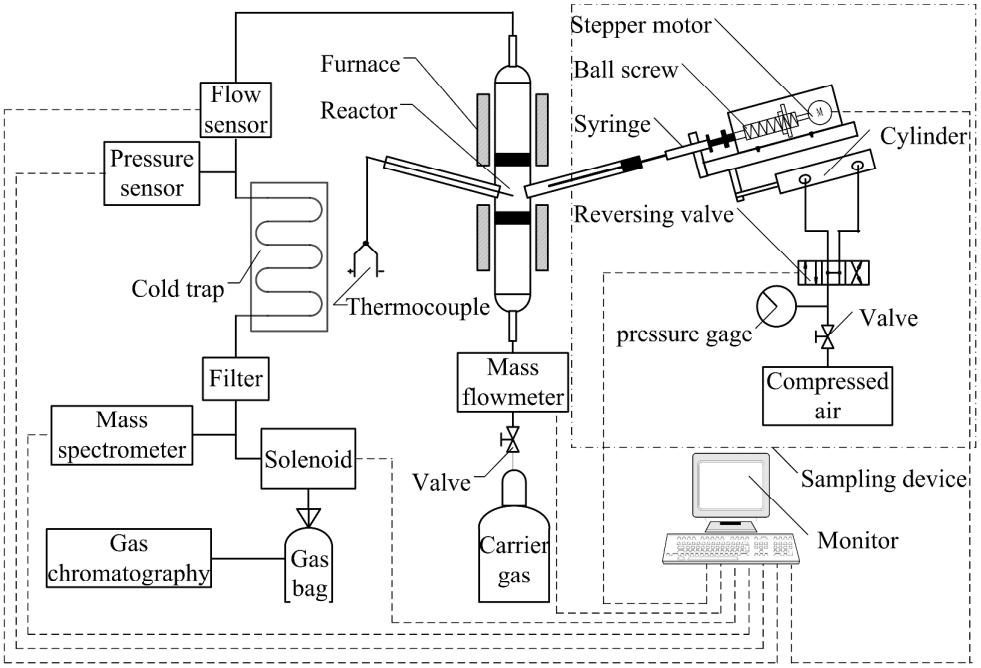

Fig. 1 Schematic diagram of the apparatus

Before each test, four grams of quart sand with particle size of 40-70 mesh were loaded into both the lower layer and upper layer of the reactor as bed material. Injection pump and syringe were pushed to the predetermined position together by the cylinder as

soon as the measured temperature reached the set value, and then the injection pump pushed the syringe piston to inject 0.05 ml tar into the reactor. After sampling the injection pump and syringe were pulled back to the appropriate location. The whole process was completed within 1 s. Throughout the experiment the syringe needle would not completely pulled out of the sealing plug in order to avoid leak through the pinhole of the sealing plug.

For the sake of evaluating the experiment system, carbon balance and carbon conversion at various temperatures were investigated. The tar firstly cracked in argon at the flow rate of 400 ml/min, and then was switched to the oxygen atmosphere (300ml/min) for combustion after cracking reaction completed to measure the carbon in solid products. The producer gas was monitored through rapid process mass spectrometry (Ametek, LC-D) on-line after the liquid products were separated in the cold trap. The rest exhaust of cracking and combustion were collected by gas collecting bags separately and then analyzed in a gas chromatography (Agilent 3000A) offline after the experiments. According to Fagbemi et al.[14], modelling the tar cracking phenomenon is of interest above 773 K (the operating temperature of an industrial gasifier), hence the reaction temperatures were predetermined as 973 K, 1023 K, 1073 k, 1123 K and 1173 K, respectively. Three parallel tests were conducted at each experimental condition to ensure the repeatability of experiments.

3. Result and Discussion

3.1. Experimental system evaluation

The composition of tar is extremely complex, and the cracking reactions of some components also produce some new liquid products, so it is difficult to calculate the conversion of tar exactly. According to Yoon et al.[15], tar cracking reactions are mostly associated with the breaking of C-C bonds and C-H bond. It also can be seen from Table 1 that carbon is the highest content element in the tar. Moreover, carbon is still the primary element in the unconverted tar. Therefore, the carbon conversion can roughly reflect the tar cracking degree. Obviously, the producer gas was the main concerns of tar removal. Therefore, in the present study carbon conversion was used to evaluate the tar conversion and was defined as:

$$\eta = n_{cg} / n_{cs} * 100\% \quad (1)$$

Where, n_{cg} is the carbon moles in the producer gas, which can be calculated according to the volume of producer gas and the chromatographic data, n_{cs} represent the carbon moles in the sample.

Table 2 test of carbon conversion and balance of tar cracking in MFBRL

Test	Conversion (%)					Balance (%)				
number	973 K	1023 K	1073 K	1123 K	1173 K	973 K	1023 K	1073 K	1123 K	1173 K
1	26.66	31.25	36.76	44.65	51.74	98.81	99.31	99.43	102.0	97.45
2	25.38	30.37	36.34	44.18	52.46	96.04	103.2	97.84	97.93	101.31
3	26.16	30.74	36.42	45.42	52.73	97.23	97.51	95.22	96.71	99.24
Average	26.07	30.79	36.51	44.75	52.31	97.36	100.01	97.50	98.88	99.33

The measured carbon conversions and balances at various temperatures are listed

in Table 2. The experimental datum showed extremely good stability and reproducibility, demonstrating good reliability of the measurement in the MFBRL. The carbon conversion increased with the increasing temperature, indicating that tar cracking degree deepened. As the temperature rose, some stable components began to crack gradually because of the availability of more energy. Moreover, the liquid intermediate products and parts of macromolecule gas were also converted into small molecular (H_2, CO, CH_4 and so on) through secondary reaction. Thus carbon in terms of gaseousness increased with the temperature rose. Carin et al. [16] studied the catalytic tar decomposition with dolomite and silica in different combinations in range of 973-1173 K and they observed that increasing temperature promoted the tar conversion, which is consistent with the results of this work. Anis and Zainal[17] observed that the tar conversion reached about 50% at 1173 K through thermal treatment, but reached up to 97% through dolomite catalytic treatment, which was much higher than the carbon conversion obtained in this work. Except for the difference between the properties of the samples, the poor catalytic performance of quartz sand (bed material in this study, whose major components is silica) cannot be neglected. According to Dou et al.[18], the silica shows much poorer catalytic activation compared to other catalysts (Y-zeolite, NiMo catalyst, alumina and lime) for 1-Methylnaphthalene cracking. El-Rub et al.[19] concluded that the least catalysts activity for phenol conversion among the six catalysts (nickel, dolomite , used fluid catalytic cracking (FCC) catalyst , commercial biomass char , olivine , silica sand)is silica sand, as well as for naphthalene conversion. Taking into account of these

differences, the carbon conversion can be deemed comparable to that thermal cracking method reported in the literatures.

The temperature and pressure drop profile for a typical experiment at 1023K are presented in Fig. 2. It is apparent that the temperature and pressure drop in MFBRL retained almost steady state with the fluctuation of measuring data within 1K and 400 Pa, respectively. It implies that the experimental condition was stable and isothermal condition was achieved.

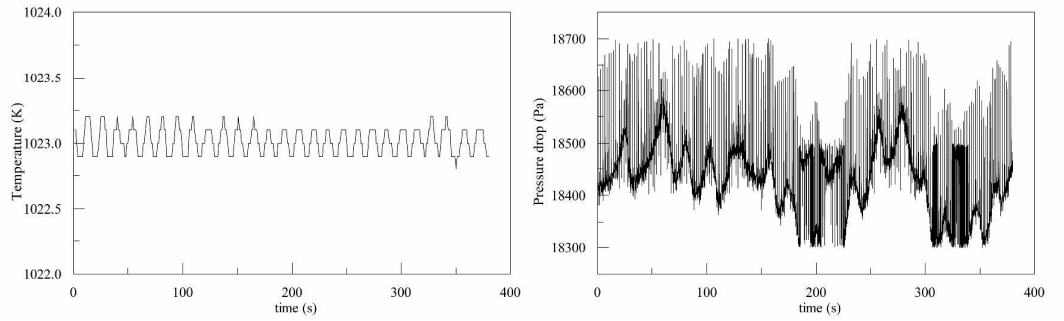

Fig. 2 Temperature and pressure drop of the reactor at 1023K

3.2. Characteristic of tar cracking

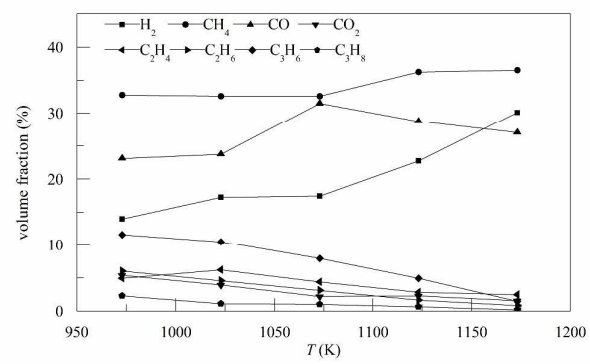

Fig. 3 Gas distribution of tar cracking in MFBRL

The chromatographic results of the producer gas of tar cracking in 973-1173 K are listed in Fig. 3 (corrected after excluding the carrier gas). It can be observed that H_2

content increased significantly with the increase of temperature. CH_4 content almost kept constant below1073K and then increased slightly. CO content increased firstly and then decreased, reaching its peak at 1073 K. In addition, CO_2 and C_2H_4, C_2H_6, C_3H_6, C_3H_8 content all presented downward trend with the increasing temperature. During tar cracking process, H_2 is mainly produced by the dehydrogenation and the cracking of macromolecular alkanes and olefins. The increasing temperature is favorable for not only the above-mentioned cracking reactions but also the secondary reactions of the intermediate products. In addition, the polycondensation reaction of aldehyde and ketone compounds in tar also produces hydrogen. The polycondensation reactions were enhanced by increasing reaction temperature as well. As a result, more free H radicals were generated, resulting in the increase of H_2 content. CH_4 becomes unstable and tends to decompose at above 873 K. In tar cracking, CH_4 is basically generated through demethylation, chain scission and arylation polycondensation of C_2 and above compounds. However, these reactions are not intensive enough to overwhelm the decomposition of CH_4 at below 1073 K. The above reactions are enhanced remarkably from 1073 K and produced more H radicals and methyl, leading to slight rise of CH_4 content. CO is mainly generated through the breaking and rearrangement of C-O and C=O bonds in aldehydes, ketones and acids and other organics. The carboxyl and carbonyl in these substances become less stable at higher temperature and tend to form a stable molecular structure through breaking carbon oxygen double bond or remove carbonyl by way of reforming and isomerization, accompanying with release of large

amounts of CO[20]. On the other hand, the water-gas reaction, which can be described as: $CO+H_2O=CO_2+H_2$, also is accelerated due to the availability of more energy and the increasing concentration of CO. The CO content reached its peak at around 1073 K, implying the balance of the two kinds of reaction is achieved. Carboxylic acid is very unstable and carboxyl is prone to crack and reform at high temperature. Besides CO, carboxyl cracking releases CO_2 as well[21], and is the main approach of CO_2 formation in tar cracking. At high temperature, CO_2 tends to react with the intermediate products and carbon deposit, resulting in the decline of CO_2 content. The aliphatic hydrocarbon such as C_2H_4, C_2H_6, C_3H_6 and C_3H_8 is the products of the cracking and reforming reactions. Although the these reactions is enhanced by increasing reaction temperature, the aliphatic hydrocarbons of C_2 or above become less stable and tend to split into CH_4 even C and H_2. In the experimental temperature range, decomposition of aliphatic hydrocarbons was dominant, which accounted for the content of hydrocarbon except CH_4 decreased with increasing temperature.

By comparing the datum in Fig. 3, it can be observed that H_2, CH_4 and CO were the major components in the producer gas, and the total volume fraction of them increased from 69.85% at 973 K to 93.62% at 1173 K. Since CO_2 content is very low while the other components are all combustible gas, the heating value of the producer gas is higher than the common biogas.

3.3. Kinetic analysis of tar cracking

As mentioned above, the major components of the producer gas are H_2, CH_4 and

CO, the total volume fractions of which are much higher than other groups. Hence, kinetic analysis for individual gas only concentrates on the mentioned three gases.

3.3.1. Theory

The relative conversion *x* at time *t* can be calculated by

$$x = \frac{\int_{t_0}^{t} c_i \times u dt}{\int_{t_0}^{t_a} c_i \times u dt} \quad (2)$$

Where, C_i is the measured concentration of gas product *i*, *u* denotes the flow rate of the gas in the outlet of the MFBRL, t_0 and t_a represent the start time and end time of pyrolysis, respectively.

Tar cracking is a complicated process, and the first order model is hard to describe the whole process. Therefore, the following model function is adopted:

$$f(x) = (1-x)^n \quad (3)$$

So the reaction rate equation can be written as:

$$dx/dt = k(T) * (1-x)^n \quad (4)$$

Where, *f(x)* is the differential form model function, *k(T)* is the reaction rate constant, *T* is the thermodynamic temperature and *n* is the reaction order.

Taking the logarithm of both sides of Eq. (4) results in the following expression:

$$\ln(dx/dt) = \ln(k(T)) + n\ln(1-x) \quad (5)$$

Eq. (5) shows a linear equation correlating *ln(dx/dt)* and *ln(1-x)*, the intercept and slope of which correspond to *ln(k(T))* and the reaction order *n*, respectively.

Taking the logarithm of Arrhenius equation, the following linear equation is obtained:

$$\ln k(T) = \ln(A) - E/RT \quad (6)$$

Where, A is the pre-exponential factor, E is apparent activate energy and R is the universal gas constant. Obviously, the apparent activation and the pre-exponential factor can be calculated according to the intercept and slope of the regression line.

3.3.2. Variation of reaction order

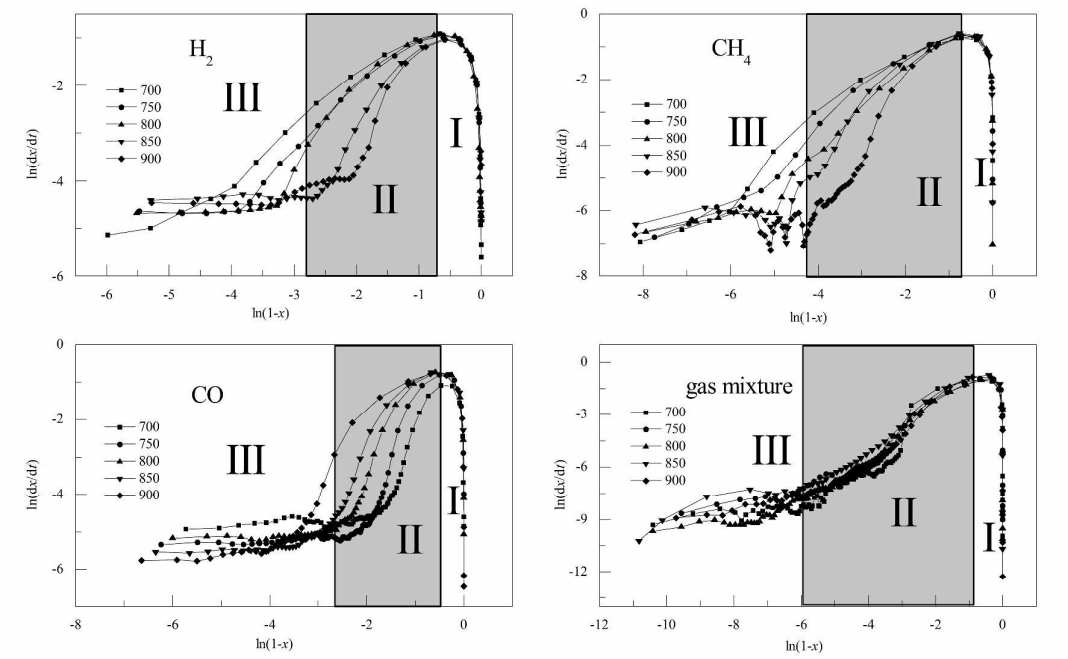

Fig. 4 Correlation of ln(dx/dt) and ln(1−x) for producer gas in MFBRL

Based on the above method, the derived curves of *ln(dx/dt)* versus *ln(1-x)* at different temperatures for producer gas are illustrated in Fig. 4. It can be observed that the curves at a given temperature can be divided into three segments, corresponding to the three reaction stages: the rapid heating stage (□), the chemical reaction control stage (□) and the termination stage (□). It can be seen from Fig. 4 that the tar conversion was very low in the rapid heating stage, indicating that the heating rate in MFBRL was flash. Hence, the mass loss before the predetermined temperature can be neglected. Obviously,

the chemical reaction control stage was the major segment of tar cracking. In this stage, the reaction rate was mainly controlled by chemical reactions because the diffusion effect was allowed to be negligible due to the good mass transfer. The curves showed good linearity and thus can represent the intrinsic cracking process. Therefore, the kinetics analysis aimed at only this stage. In the termination stage the reaction rate was very low and was mainly controlled by internal diffusion. The reaction rate constants and reaction orders of the major components (H_2, CH_4, CO) and their mixture were calculated according to Eq. (5) and the results were listed in Table 3. It can be seen that the values of the linear correlation coefficient R^2 for all the curves were above 0.96, indicating the good reliability of the experimental results.

Table 3 Rate constant and reaction order of the main gas component in MFBRL

		Temperature				
		973 K	1023 K	1073 K	1123 K	1173 K
H_2	ln(k(T))	-0.004	0.398	0.633	1.031	1.343
	n	0.971	1.270	1.475	2.037	2.504
	R^2	0.985	0.989	0.969	0.976	0.975
CH_4	ln(k(T))	0.331	0.773	1.120	1.461	1.775
	n	0.912	1.086	1.364	1.593	2.013
	R^2	0.965	0.974	0.980	0.962	0.977
CO	ln(k(T))	0.210	0.759	1.280	1.898	2.282
	n	2.681	2.678	2.441	2.398	2.075
	R^2	0.965	0.967	0.972	0.978	0.977
Gas mixture	ln(k(T))	-0.458	0.043	0.471	0.800	1.173
	n	1.410	1.437	1.514	1.461	1.762
	R^2	0.973	0.972	0.976	0.989	0.969

It can be observed from Table 3 that all the reaction orders varied with the

variation of reaction temperatures rather than kept constant. According to Eq. (3), it can be concluded that the reaction mechanism varied at different temperatures. The application of first-order reaction models in tar cracking kinetics has become almost formulaic in many previous literatures[22- 24]. In these literatures, the model of tar cracking was always considered to be a first order function with respect to the remaining non-cracked tar. But their assumption was uncritical and just occurred in the context of no strict verification and insufficient understanding of their fundamental limitations, always leading to lower parameters[25]. In a complicated reaction process, the reaction order obtained is just a combined reflection of a series of reactions. Tar cracking comprises a series of very complex inhomogeneous reactions, of which the complexity increases as tar conversion and molecular weight of components increase. The fluctuation of reaction order for CO were much smaller than H_2, indicating that there were less precursors for formation of CO. The reaction orders for H_2 varied greatly, implying that there were many precursors to generate H_2. A variety of reactions of different difficulty were superimposed together, so that the reaction order of H_2 fluctuated greatly. The reaction orders for gas mixture showed good convergence maybe due to the coupling effect of different groups.

3.3.3. Apparent activation energy and pre exponential factor analysis

The *ln(k(T))* of MFBRL experiments listed in Table 3 were correlated with 1000/*T* and the results were plotted in Fig. 5. The results can be considered to be reliable, based on the good linearity of correlation coefficient above 0.99 for all the correlation curves

in Fig. 5. The pre-exponential factors for formation of H_2, CH_4 and CO range from $2.37*10^3$ S^{-1} to $2.87*10^5$ S^{-1}, and in order the apparent activation energies were 62.96 kJ/mol, 67.89 kJ/mol and 100.2 kJ/mol, respectively. The discrepancy between the apparent activation energies may be explained by the difficulty of the reactions for forming the gas component. As is well known, the chemical reaction is bound to break chemical bonds, and more energy is required to overcome the barrier of the reaction when the chemical bond is firmer. That is to say, the firmer chemical bond means the higher activation energy. It can be known that the generation of H_2 is mainly associated with the breaking of C-H bond, while the generation of CH_4 is mainly related to C-C or C=C bond breaking. CO is basically released through decomposition of carboxyl and carbonyl, which usually correspond to C=O bond breaking. The average bond energies of C-H, C-C, C=C and C=O are 414 kJ/mol, 332 kJ/mol, 611 kJ/mol and 728 kJ/mol, respectively[26]. Obviously, the average bond energy of C=O bond is much higher than the rest, so there is no wonder that the apparent activation energy for CO is greater than other gas components. Although the average bond energy of C-C bond is slightly lower than C-H bond, the average bond energy of C=C bond is far outweigh that of C-H bond. The combined effect of the two kinds of chemical bonds results in the higher apparent activation energy of CH_4 compared to H_2. Besides, the polarity of C-H makes it easier to break.

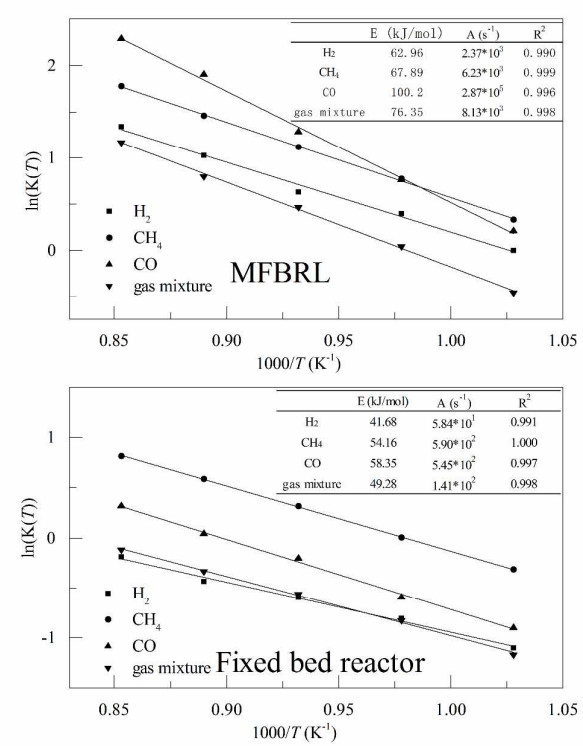

Fig. 5 Linear fitting of ln(k(*T*)) versus 1000/*T* for gas components in MFBRL and fixed bed experiments

For the gas mixture, the apparent activation energy and pre-exponential factor were 76.35 kJ/mol and $8.13*10^3$ S^{-1}, respectively. For the kinetic parameters derived with a new method, it is significant to compare the results with the literatures. Dou et al.[18] reported that the activation energy around 66.6 and 37.2 kJ/mol for cracking of 1-Methylnaphthalene using NiMo or Y-zeolite as catalyst. El-Rub et al.[19] investigated naphthalene conversion in the temperature range 973–1173 K (commercial biomass char as catalyst) and obtained an apparent activation energy of 61 kJ/mol and pre-exponential factor of 1.0*104 s^{-1}. According to Devia et al.[24], activation energy for model compounds such as benzene, naphthalene are usually much higher than that

reported for real tar. However, the apparent activation energies for model compounds in the literatures were much lower than that for real tar in this study, indicating the poor catalytic property of quart sand. For the real tar removal reaction, an E of 51 kJ/mol and A of 14,476 (m^3 (Tb, wet)/kg h) for nickel-based catalysts was reported by Lv et al.[27]. Delgado et al.[28] concluded that the apparent activation energies for tar elimination using cheap calcined minerals or rocks downstream from the bubbling fluidized bed biomass gasifier are in the range of 42-47 kJ/mol. However, the results obtained through thermal cracking were somewhat higher. Caballero et al.[29] conducted an experiment on cracking of kraft lignin tar and concluded that the activation energy was 84.7 kJ/mol while the pre-exponential factor was 4.138×10^3 S^{-1}. Stiles and Kandiyoti[30] reported that the apparent energy and pre-exponential factor for cellulose tar were 81 kJ/mol and 7.9×10^3 S^{-1}, respectively; for silverbirch tar, the results were 73 kJ/mol and 5.3×10^3 S^{-1}, respectively. These results are remarkably close to the conclusion of this study. As a matter of fact, due to the different sources of raw materials, there are great differences among the chemical composition of samples; in addition, the discrepancy among experimental conditions (reactor and reaction temperature and so on) and computing method also affect the results to some extent. Taking into account of the difference of the experiments, the results obtained in this study can be considered as comparable to most of the literatures.

3.3.4. Fixed bed experiments

In order to further evaluate the performance of the experimental system, it is of

interest to eliminate the interference caused by varied samples. Parallel experiments using the same sample were conducted in a fixed bed system under the same temperatures. With the same calculation method, reaction orders and apparent activation energies were deduced and illustrated in Table 4 and Fig. 5.

Table 4 rate constant and reaction order of the main gas component in fixed bed experiments

		Temperature				
		973 K	1023 K	1073 K	1123 K	1173 K
H_2	ln(k(T))	-1.102	-0.806	-0.597	-0.434	-0.190
	n	1.476	2.031	1.985	2.124	2.019
	R^2	0.961	0.987	0.983	0.993	0.994
CH_4	ln(k(T))	-0.317	0.002	0.316	0.588	0.816
	n	1.314	1.481	1.615	1.694	1.867
	R^2	0.988	0.983	0.983	0.967	0.971
CO	ln(k(T))	-0.902	-0.598	-0.210	0.041	0.316
	n	1.335	1.590	1.652	1.702	1.483
	R^2	0.967	0.973	0.966	0.961	0.997
Gas mixture	ln(k(T))	-1.167	-0.827	-0.563	-0.332	-0.119
	n	1.190	1.300	1.596	1.815	1.957
	R^2	0.966	0.992	0.976	0.962	0.995

Similar to the MFBRL experiments, the derived reaction orders varied greatly rather than kept constant. Compared the datum in Fig. 5, it can be observed that the apparent activation energies obtained from fixed bed experiments are lower than the counterparts from MFBRL experiments. Considering the experimental condition was exactly the same except the flow rate of carrier gas, it can be concluded that the difference was mainly caused by diffusion. According to Arrhenius equation, lower

apparent activation energy means bad temperature sensitivity. Therefore, the higher values of apparent activation energy deduced in MFBRL experiments demonstrate that the reactions in the MFBRL are more sensitive to temperature. In the MFBRL experiments, good mass and heat transfer are allowed as a result of higher flow rate, thus the reaction rate was mainly controlled by chemical kinetics. However, in the fixed bed experiments, reactions were vulnerable to be inhibited by diffusion owing to bad external diffusion. Consequently, with the increase of temperature, the reaction rate in the fixed bed reactor accelerated more slowly than in a MFBRL. That is to say, the sensitivity of reactions to temperature decreased in the fixed bed experiments. According to discussion above, it can be concluded that better mass and heat transfer were achieved in MFBRL and the deduced kinetic parameters were closer to the intrinsic ones. Generally speaking, benefiting from the minimized inhibition and rapid heating, the obtained kinetic parameters in MFBRL can provide a better description of the true reaction mechanism. Obviously, in the kinetics study of a volatile liquid, MFBRL has particular advantages compared to fixed bed.

4. Conclusions

In tar cracking, it's observed that H_2, CH_4 and CO account for the majority of producer gas and the total volume fraction of them reached 93.62% at 1173 K. The reaction orders varied greatly with the variation of temperature, suggesting that temperature significantly affected the reaction mechanism. The pre-exponential factors for H_2, CH_4, CO and gas mixture were in the range of $2.37*10^3$-$2.87*10^5$ S^{-1}, while the

apparent activation energies of them ranged from 62.96-100.2 kJ/mol. The derived results in MFBRL were obvious higher than in fixed bed, indicating the obtained parameters were closer to the intrinsic ones.

Acknowledgements

The authors grateful appreciate the financially support from the National Special Project for Development of Major Scientific Equipment (2011YQ120039). Assistances of Ms. Junrong Yue from Chinese academy of science on experiments are also acknowledged.

References

1 U. Oemar, M. L. Ang, K. Hidajata and S. Kawi, RSC Adv., 2015, **5**, 17834-17842.

2 D. Li, M. Koike, J. Chen, Y. Nakagawa and K. Tomishige, Int. J. Hydrogen Energ., 2014, **39**(21), 10959-10970.

3 S. Anis and Z. A. Zainal, Renew. Sust. Energ. Rev., 2011, **15**(5), 2355-2377.

4 Y. Shen, C. Areeprasert, B. Prabowo, F. Takahashi and K. Yoshikawa, RSC Adv., 2014, 4, 40651-40664.

5 H. J. Park, S. H. Park, J. M. Sohn, J. Park, J. K. Jeon, S. S. Kim and Y. K. Park, Bioresour. Technol., 2010, **101**(1), S101-S103.

6 M. Kong, Q. Yang, J. Fei and X. Zheng, Int. J. Hydrogen. Energ., 2012, **37**, 13355-13364.

7 F. C. Diego, G. B. Alberto, N. Susanna and O. Pedro, Chem. Eng. J., 2013, **228**, 1223-1233.

8 D. Li, M. Tamura, Y. Nakagawa and K. Tomishige, Bioresour. Technol., 2015, **178**, 53-64.

9 B. Dou, W. Pan, J. Ren, B. Chen, J. Hwang and T. Yu, Energ. Convers. Manage., 2008, **49**(8), 2247-2253.

10 J. Yu, C. Yao, X. Zeng, S. Geng, L. Dong, Y. Wang, S. Gao and G. Xu, Chem. Eng. J., 2011, **168**, 839–847.

11 J. Yu, X. Zeng, J. Zhang, M. Zhong, G. Zhang, Y. Wang and G. Xu, Fuel, 2013, **103**, 29-36.

12 J. Yu, J. Yue, Z. Liu, L. Dong and G. Xu, AICHE J., 2010, **56** (11), 2905-2912.

13 Y. Mao, L. Dong, Y. Dong, W. Liu, J. Chang, S. Yang, Z. Lv and P. Fan, Bioresour. Technol., 2015,**181**, 155-162.

14 L. Fagbemi, L. Khezami and R. Capart, Appl. Energ., 2001, **69** (4), 293-306.

15 S. J.Yoon, Y. C. Choi and J. G.Lee, Energ. Convers. Manage., 2010, **51**(1), 42-47.

16 C. Myrén, C. Hörnell, E. Björnbom and K. Sjöström, Biomass Bioenerg., 2002, **23**, 217 - 227.

17 S. Anis and Z. A. Zainal, Bioresour. Technol., 2013, **150**, 328-337.

18 B. Dou , J. Gao , X. Sha and S. W. Baek, Appl. Therm. Eng., 2003, **23**, 2229-2239.

19 Z.A. El-Rub, E.A. Bramer and G.Brem, Fuel, 2008, **87**, 2243-52.

20 H. Tan, PhD thesis, Zhejiang University, 2005.

21 Y. C. Lin, J. Cho, G. A. Tompsett, P. R. Westmoreland and G. W. Huber, J. Phys. Chem. C, 2009, **113**(46), 20097-20107.

22 P. Morf, P. Hasler and T. Nussbaumer, Fuel, 2002, **81**(7), 843-853.

23 J. Rath, G. Steiner, M. G. Wolfinger and G. Staudinger, J. Anal. Appl. Pyrol., 2002, **62**(1), 83-92.

24 L. Devi, K. J. Ptasinski, F. J. J. G. Janssen, S. V. B. Van Paasen, P. C. A. Bergman and J. H. A. Kiel, Renew. Energ., 2005, **30**(4), 565–587.

25 J.Corella, J. M. Toledo, and M.P. Aznar, Ind. Eng. Chem. Res., 2002, **41**, 3351-3356.

26 M. L. Li, Concise Handbook of Chemical Data, Chemical Industry Press, Beijing, China, 2003.

27 P. Lv, Z. Yuan, C. Wu, L. Ma, Y. Chen and N. Tsubaki, Energ. Convers. Manage., 2007, **48**, 1132-1139.

28 J. Delgado, M.P. Aznar and J. Corella, Ind. Eng. Chem. Res., 1997, **36**, 1535-1543.

29 J. A. Caballero, R. Font and A. Marcilla, J. Anal. Appl. Pyrol., 1996, **38**(0), 131-152.

30 H. N. Stiles and R. Kandiyoti, Fuel, 1989, **68** (3), 275-282.